Cellular Immunology 393–394 (2023) 104782

Contents lists available at ScienceDirect

Cellular Immunology

journal homepage: www.elsevier.com/locate/ycimm

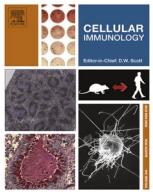

Antitumor activity of pegylated human interferon β as monotherapy or in combination with immune checkpoint inhibitors via tumor growth inhibition and dendritic cell activation

Rui Wang [a,1], Tao Zhang [a,1], Yuan Lu [a,1], Yalong Lin [a], Shuyuan Kou [a], Xuefeng Li [a], Yang Wang [a], Liangzhi Xie [a,b,c,*]

[a] Beijing Engineering Research Center of Protein and Antibody, Sinocelltech Ltd., Beijing 100176, China
[b] Beijing Key Laboratory of Monoclonal Antibody Research and Development, Sino Biological Inc., Beijing 100176, China
[c] Cell Culture Engineering Center, Chinese Academy of Medical Sciences & Peking Union Medical College, Beijing 100005, China

ARTICLE INFO

Keywords:
Pegylated human interferon β
Antitumor therapy
Immune checkpoint inhibitors
Pegylated human interferon α

ABSTRACT

Type I interferons (IFN), especially human IFN alpha (IFNα), have been utilized for antitumor therapy for decades. Human interferon beta (IFNβ) is rarely used for cancer treatment, despite advantages over IFNα in biological activities such as tumor growth inhibition and dendritic cell (DC) activation. The utilization of pegylated human IFNβ (PEG-IFNβ), as monotherapy or in combination with immune checkpoint inhibitors (ICIs) was evaluated in this study through in vivo efficacy studies in syngeneic mouse melanoma, non-small cell lung cancer (NSCLC), and colon adenocarcinoma (COAD) models resistant to immune checkpoint inhibitors (ICIs). In vitro comparative study of PEG-IFNβ and pegylated IFNα-2b was performed in terms of tumor growth inhibition against human melanoma, NSCLC and COAD cell lines and activation of human monocyte-derived DCs (MoDCs). Our data demonstrate that the in vivo antitumor effects of PEG-IFNβ are partially attributable to tumor growth-inhibitory effects and DC-activating activities, superior to pegylated IFNα-2b. Our findings suggest that utilizing PEG-IFNβ as an antitumor therapy can enhance the therapeutic effect of ICIs in ICI-resistant tumors by directly inhibiting tumor growth and induction of DC maturation.

1. Introduction

Immune checkpoint inhibitors (ICIs), such as anti-programmed cell death protein 1/anti-programmed cell death 1 ligand 1 (PD-1/PD-L1) monoclonal antibodies, have made great success in the treatment of malignancies. Achievements in non-small-cell lung cancer (NSCLC), colorectal cancer (CRC), and melanoma have resulted in durable responses [1–4]. However, limited patients benefited from such treatments due to primary or acquired resistance attributed to loss of neoantigens, defective antigen presentation, and upregulation of immune checkpoints other than PD-1/PD-L1 [5–8]. In fact, objective response rates (ORR) in patients with positive expression of the PD-L1 biomarker range from 10 % to 40 % [9–13]. Therefore, it is necessary to explore new therapeutic strategies, such as combination therapy, to overcome drug resistance to ICIs.

Type I IFNs have enormous antitumor capabilities attributed to direct inhibition of tumor cell proliferation and tumor angiogenesis, as well as immunomodulatory effects [14–17]. Emerging evidence suggests that type I IFNs can significantly induce tumor cell apoptosis and inhibit tumor cell proliferation and metastasis [15,18]. In addition, type I IFNs stimulate dendritic cell (DC) differentiation and maturation, thereby enhancing DC activity [19]. Adequate type I IFN promotes DC activation and T cell cross-priming [20]. Thus, type I IFNs may be ideal collaborators for ICIs to enhance the therapeutic efficacy, especially in subpopulations of cancer patients with deficient antigen presentation and T cell priming.

Among the subtypes of type I IFNs, interferon alfa (IFNα) and Pegylated interferon alfa (PEG-IFNα) are of interest. IFNα [21] and PEG-IFNα [22,23] have been approved for the treatment of cancer. Compared to IFNα, another member of type I IFNs, interferon beta (IFNβ) exhibits better antitumor potency which correlates with more potent receptor binding, DC activation and antiproliferative activity [24–29]. In the

* Corresponding author at: No.31 Kechuang 7th Street, BDA, Beijing 100176, China.
E-mail address: LX@sinocelltech.com (L. Xie).
[1] Contributed equally.

https://doi.org/10.1016/j.cellimm.2023.104782
Received 17 May 2023; Received in revised form 10 October 2023; Accepted 30 October 2023
Available online 3 November 2023

clinical setting, IFNβ and pegylated interferon beta (PEG-IFNβ) have been approved as disease-modifying therapies for multiple sclerosis (MS) [30,31]. To date, IFNβ monotherapy, with moderate efficacy mainly through early phase studies [32,33] and ongoing phase III clinical trials [34], is approved only in Japan for the treatment of cancer [35]. The potency of IFNβ in combination with ICIs has been explored preliminarily in clinical trials in melanoma patients [36] and preclinical studies of mouse IFNβ in murine melanoma models [37,38]. A comprehensive preclinical elucidation of the efficacy of IFNβ as monotherapy or in combination with ICIs in tumor models other than melanoma is warranted.

In this study, human IFNβ was conjugated with polyethylene glycol (named PEG-IFNβ) to conquer the deficiencies of cytokine-based therapies, such as rapid clearance and short half-life [39,40]. The efficacy of PEG-IFNβ as monotherapy or in combination with anti-PD-1 antibody in lung cancer, colon cancer, and melanoma mouse models was elucidated. In addition, we compared the effect of PEG-IFNβ and pegylated human IFNα-2b (PEG-IFNα-2b) on proliferation of human tumor cell lines (lung cancer, colon cancer, and melanoma) and activation of human monocyte-derived dendritic cells (MoDCs).

2. Materials and methods

2.1. Cells

Mouse LLC, MC38, B16F1 cells and human A549, A375, HCT116 cells were bought from American Type Culture Collection (ATCC, USA), and cultured in Dulbecco's modified Eagle's medium (SinoCellTech Ltd., China) supplemented with 10 % fetal bovine serum (Gibco, USA) at 37℃. Human MoDCs were generated from peripheral blood mononuclear cells (PBMCs) (Oribiotech, China) cultured in RPMI (SinoCellTech Ltd., China) and 10 % FBS (Gibco, USA) at 37℃, supplemented with 20 ng/mL GM-CSF (R&D Systems, USA) and 160 ng/mL IL-4 (Sino Biological Inc., China). Expression of cell surface molecules was detected after treatment with PEG-IFNβ (SinoCellTech Ltd., China) or PEG-IFNα-2b (Amoytop, China) for 72 h.

2.2. Mice

Female C57BL/6 mice (6——8 weeks) were purchased from Beijing Charles River Laboratory Animal Technology Co., Ltd. Human PD-1 knock-in mice (C57BL/6 background) were purchased from Beijing Biocytogen Co., Ltd. All animal experiments comply with Chinese animal use guidelines and the procedures were approved by the Committee of Laboratory Animal Welfare and Ethics of the National Institutions for Food and Drug Control [No. 2019(B) 001].

2.3. Evaluation of in vivo biological activity of PEG-IFNβ in mice

C57BL/6 mice received a single subcutaneous (s.c.) injection of PEG-IFNβ or mouse IFNβ (PBL Assay Science, USA). Mouse sera were collected at 0, 2, 24 and 48 h, followed by flow cytometry to determine the expression levels of chemokines downstream of IFNβ, such as CXCL1, CXCL9, CXCL10, and CCL2 [17,41–46].

2.4. Syngeneic tumor models

Mice were subcutaneously inoculated with 1.5×10^6 LLC cells, 1.0×10^6 B16F1 cells, and 1.0×10^6 MC38 cells in 100 uL of PBS into the right dorsal flank. Tumor volumes were calculatd as follows: volume (mm^3) = (width × $length^2$) / 2. Tumor growth inhibition ratio (TGI) was calculated as follows: TGI (%) = $(1\text{-}V_t / V_v) \times 100$ %. V_t: tumor volume in the treatment group; Vv: tumor volume in the vehicle group. When tumor volumes reached 50——100 mm^3, mice were subjected to treatment with PEG-IFNβ (s.c.), anti-human PD-1 antibody (SCTI10A, SinoCellTech Ltd) or anti-mouse PD-1 antibody (BioXcell, USA) injected intraperitoneally (i.p.), or combination therapy. Dosages and treatment intervals were shown in figure legends.

2.5. Immunohistochemistry

Mouse tumor tissues were fixed in 4 % paraformaldehyde (Sigma, USA) for 24 h, dehydrated and cleared in xylene (Sinopharm, China). 4-μm sections were treated with 3 % hydrogen peroxide (Sinopharm, China) for 15 min, autoclaved with 0.01 mol/L EDTA (Shhushi, China) and blocked with 10 % goat serum (ZSGB-BIO, China) for 30 min at room temperature. Slides were incubated with anti-CD3 antibody (Cell Signaling Technology, USA) overnight at 4℃, stained with goat anti-rabbit secondary antibody (ZSGB-BIO, China) for 1 h, visualized with 3, 3′-diaminobenzidine (DAB) (ZSGB-BIO, China), and counterstained with hematoxylin (Njjcbio, China) at room temperature. Morphological evaluation was performed by image scanner (KFBIO, China). The IHC staining intensity for anti-CD3 antibody was semi-quantified based on a five-point scale [47,48].

2.6. Cell proliferation assay

A549, A375 and HCT116 cells were seeded in 96-well plates (Corning, USA) at a density of 5×10^3 cells/well. After 24 h, cells were treated with PEG-IFNα-2b or PEG-IFNβ for 96 h. Cells were incubated in the dark at 37℃ for 2 h in the presence of Cell Counting Kit-8 (CCK-8) reagents (10 μL/well) (Meilune, China). Absorbance at 450 nm was measured by a microplate reader (BioTex, USA). Clone formation assay was performed by crystal violet staining, and data analysis was performed with image J (National Institutes of Health, USA).

2.7. Flow cytometry

For chemokine assay, mouse sera were mixed with anti-CXCL1, anti-CXCL9, anti-CXCL10, and anti-CCL2 antibodies for further detection according to the manufacturer's instructions (CBA kit, Biolegend, USA). For tumor-infiltrating lymphocytes (TILs) assay, TILs were isolated (MACs, USA) and stained for CD49b, CD45, NK1.1, CD4, and CD8 (BD, USA). For DC activation assay, MoDCs were stained with anti-CD11c (BD, USA), anti-HLA-DR, anti-CD80, anti-CD83 and anti-CD86 antibodies (Biolegend, USA). FACS was performed using FACSCelesta (BD, USA) and analyzed with FlowJo software (FlowJo, USA).

2.8. Statistical analysis

All data were presented as mean ± standard deviation (SD). Graphpad Prism 8.0 software (GraphPad Software, USA) was used for data analysis. Comparisons between two groups were performed using unpaired *t*-test. Comparisons between multiple groups were performed by one-way analysis of variance and Tukey-Kramer test analysis. A *P* value less than 0.05 was considered statistically significant.

3. Results

3.1. In vivo biological activity of PEG-IFNβ in mice

Human IFNβ (hIFNβ) shares 49.2 % sequence identity with mouse IFNβ (mIFNβ) [49]. The receptors for type I interferons share approximately 50 % sequence identity between humans and mice [50]. To verify the feasibility of using mouse syngeneic tumor models to study the efficacy of PEG-IFNβ, we validated the biological activity of PEG-IFNβ in C57BL/6 mice. A single dose of PEG-IFNβ was injected subcutaneously into C57BL/6 mice at three dose levels (10^5 IU, 10^6 IU, and 10^7 IU). mIFNβ (0.1 mg/kg) was used as positive control. Serum levels of IFNβ downstream chemokines were measured before and after dosing at indicated time points (Fig. 1). Elevated serum levels of all tested chemokines were observed in both the PEG-IFNβ and mIFNβ treated groups.

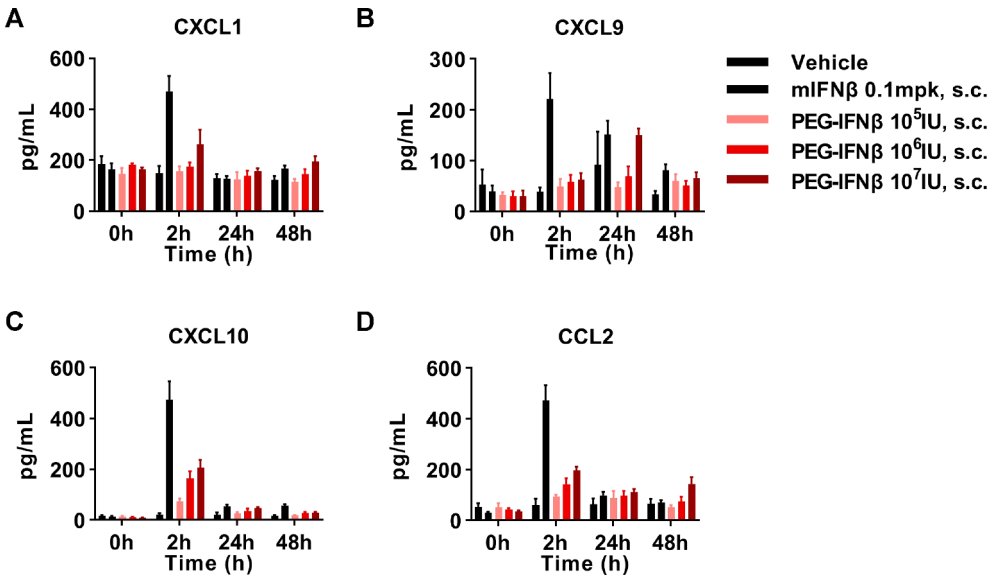

Fig. 1. Characterization of chemokine levels in mouse serum after PEG-IFNβ or mouse IFNβ treatment. C57BL/6 mice (n = 4/group) were injected subcutaneously with a single dose of PEG-IFNβ (10^5 IU, 10^6 IU, and 10^7 IU, respectively) or mIFNβ (0.1 mg/kg). Serum levels of CXCL1 (**A**), CXCL9 (**B**), CXCL10 (**C**) and CCL2 (**D**) were measured predose (0 h) and postdose (2 h, 24 h and 48 h).

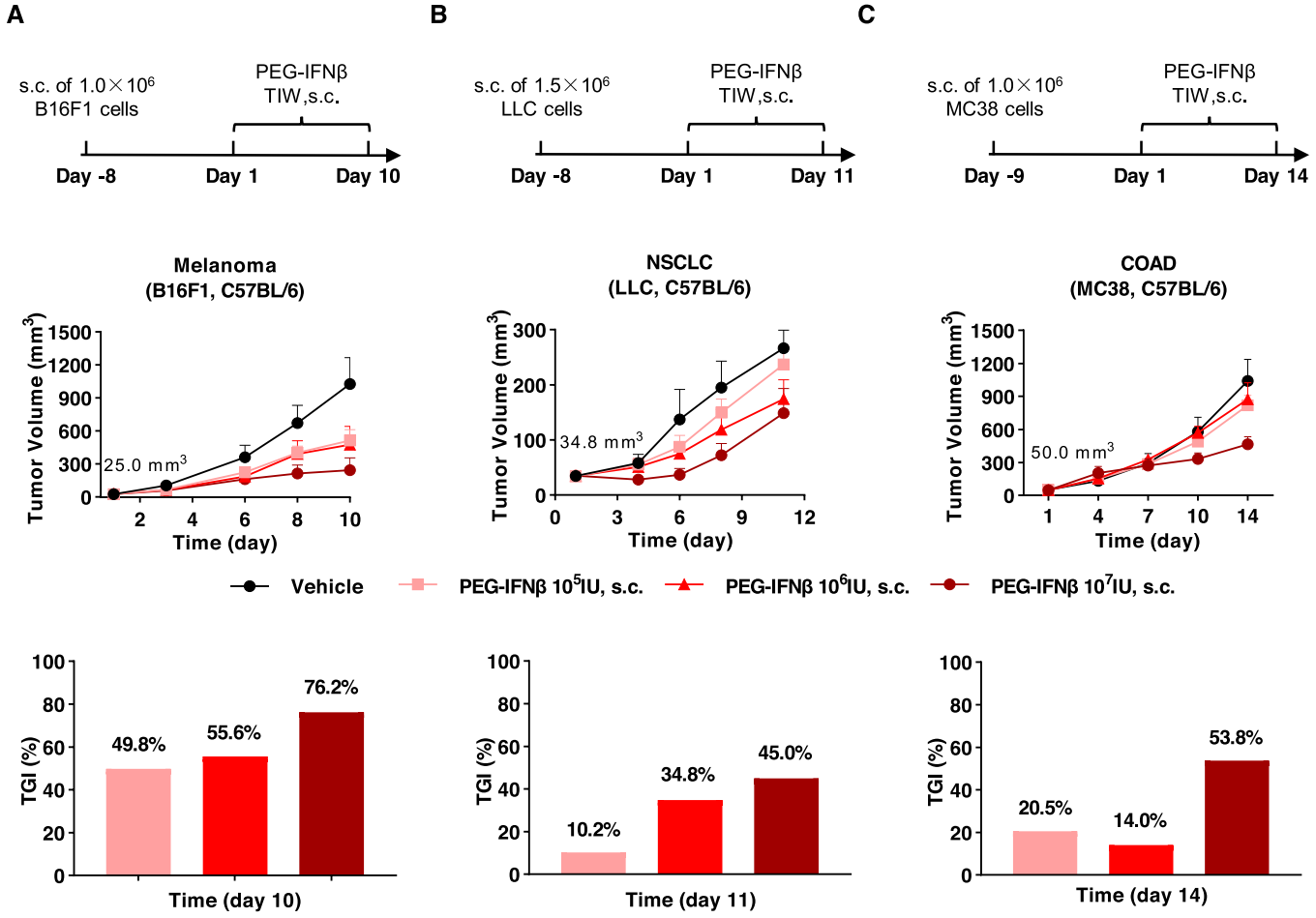

Fig. 2. Antitumor effects of PEG-IFNβ monotherapy in syngeneic mouse models of Melanoma, NSCLC and COAD. C57BL/6 mice (n = 6/group) were inoculated with B16F1 (**A**), LLC (**B**), and MC38 (**C**) cell lines, and treated with PEG-IFNβ (10^5 IU, 10^6 IU and 10^7 IU) administered subcutaneously 3 times per week. Upper panel: Tumor growth curves. Bottom panel: TGI at the end of the experiment.

Serum concentrations of CXCL1, CXCL10 and CCL2 reached peak levels 2 h after administration and gradually decreased thereafter (Fig. 1A,C, D). CXCL9 peaked at 2 h after mIFNβ administration and 24 h in the serum of PEG-IFNβ-treated mice (Fig. 1B). Therefore, PEG-IFNβ could activate the expression of chemokines downstream of mIFNβ, suggesting that syngeneic mouse tumor models were suitable for evaluating the therapeutic effect of PEG-IFNβ.

3.2. *Therapeutic effect of PEG-IFNβ in syngeneic mouse models of melanoma, non-small cell lung cancer (NSCLC), and colon adenocarcinoma (COAD)*

To evaluate the therapeutic effect of PEG-IFNβ as monotherapy, C57BL/6 mice were inoculated with the mouse melanoma cell line B16F1, the lung cancer cell line LLC, or the colorectal cancer cell line MC38, with non-inflammatory immune phenotypes or enriched immunosuppressive cells [51,52], implicating resistant to ICIs, were treated with PEG-IFNβ (10^5 IU, 10^6 IU and 10^7 IU) three times per week.

In the B16F1 melanoma tumor model, enhanced antitumor effects were observed compared to the LLC model. In the PEG-IFNβ-treated groups (10^5 IU, 10^6 IU, and 10^7 IU/dose), the TGI at the end of the experiment (day 10) were 49.8 %, 55.6 % and 76.2 %, respectively (Fig. 2A). The tumor volume in PEG-IFNβ (10^7 IU) treatment group was significantly lower than that in the vehicle group (1026.4 ± 538.1 mm^3 *vs.* 242.8 ± 225.2 mm^3, $P < 0.01$). In the LLC NSCLC tumor model, PEG-IFNβ inhibited tumor growth in a dose-dependent manner. TGI at the end of the experiment (day 11) was 10.2 %, 34.8 % and 45.0 % in mice treated with 10^5 IU, 10^6 IU and 10^7 IU of PEG-IFNβ, respectively (Fig. 2B). A significant difference in tumor volume was observed between the PEG-IFNβ (10^7 IU) treated group and the vehicle group (266.5 ± 80.3 mm^3 *vs.* 148.6 ± 109.6 mm^3, $P < 0.05$). In the MC38 COAD tumor model, TGI on day 14 for each PEG-IFNβ treated group (10^5 IU, 10^6 IU, and 10^7 IU/dose) was 20.5 %, 14.0 % and 53.8 %, comparable to those in the LLC model (Fig. 2C). PEG-IFNβ (10^7 IU) treatment lead to significantly lower tumor volume than the vehicle group (1040.0 ± 483.4 mm^3 *vs.* 464.8 ± 170.3 mm^3, $P < 0.05$).

3.3. *PEG-IFNβ enhanced the antitumor effects of anti-PD1 antibodies in syngeneic mouse models of melanoma, NSCLC, and COAD*

Next, the efficacy of PEG-IFNβ on reinforcing the therapeutic effect of the immune checkpoint blocker anti-PD-1 antibody was verified in mouse LLC, B16F1, and MC38 tumor models.

In the B16F1 model, both anti-mPD-1 antibody and PEG-IFNβ showed moderate efficacy, with a TGI of 40.6 % and 37.1 % (day 13), respectively, reaching 60 % in the combined treatment group (Fig. 3A). We further verified this effect in the LLC model. The antitumor effects of PEG-IFNβ and an anti-human PD-1 antibody (SCT-I10A), were evaluated in LLC-tumor bearing hPD-1 knock-in (KI) C57BL/6 mice as monotherapy or in combination. On day 18 after treatment, SCT-I10A

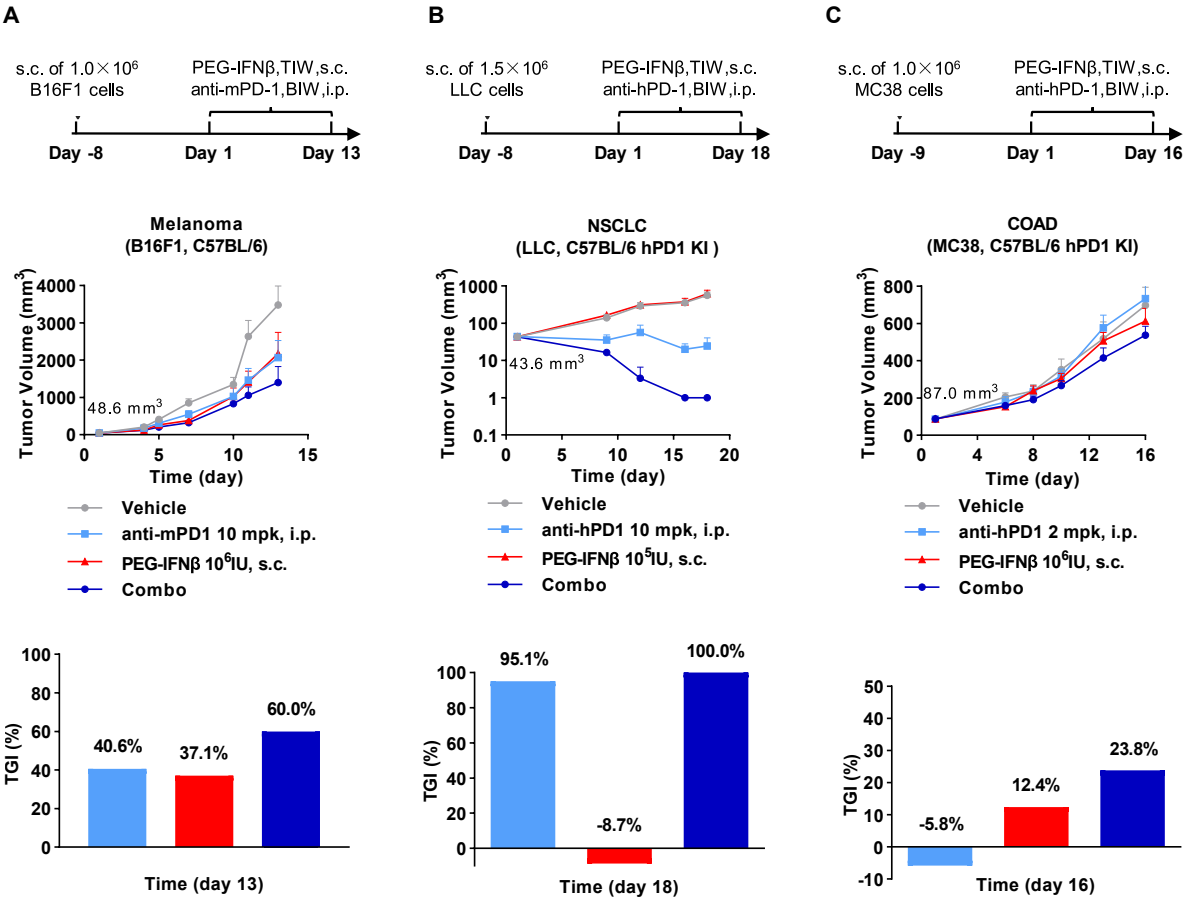

Fig. 3. Synergistic antitumor effects of PEG-IFNβ and anti-PD-1 therapeutic antibody in syngeneic mouse models of Melanoma, NSCLC, and COAD. (**A**) C57BL/6 mice bearing melanoma B16F1 (n = 6/group), (**B**) hPD-1 KI C57BL/6 mice bearing lung cancer LLC (n = 8/group), and (**C**) hPD-1 KI C57BL/6 mice bearing colorectal cancer MC38 (n = 7/group), were injected with PEG-IFNβ (s.c.) 3 times a week or anti-PD1 antibody (i.p) twice a week at indicated dose levels. Upper panel: Tumor growth curves. Bottom panel: TGI at the end of the experiment.

monotherapy (10 mg/kg) exhibited significant tumor growth inhibitory ability with a TGI of 95.1 %, while low-dose PEG-IFNβ monotherapy (10^5 IU) could hardly inhibit the growth of LLC cell line in vivo. All mice in the combination therapy group achieved a complete response (CR) from day 16 on, with a slight increase in TGI compared with anti-hPD-1 monotherapy (95.1 % *vs.* 100 %) (Fig. 3B). In the MC38 model, hPD-1 KI C57BL/6 mice bearing MC38 tumor were administered with SCT-I10A at a relatively low dose (2 mg/kg) as monotherapy or in combination with a moderate dose (10^6 IU) of PEG-IFNβ. On day 16 after treatment, the TGI for combination therapy was 23.8 %, better than that for each monotherapy group (12.4 % for PEG-IFNβ, and − 5.8 % for anti-hPD-1) (Fig. 3C).

3.4. Immunomodulatory effects of IFNβ on the tumor microenvironment of B16F1 melanoma

With the ability to inhibit melanoma cell growth and induce dendritic cells to cross-prime $CD8^+$ T cells in vitro and in vivo, IFNβ has been used clinically to treat malignant melanoma [35,45,53]. We validated the immunomodulatory effect of IFN-β on the tumor microenvironment in the B16F1 melanoma model. The ratio of $CD8^+$T/$CD4^+$T and $CD8^+$T/Treg, which indicate the potency of anti-tumor T cell immunity [54,55], showed no difference between the vehicle-treated group and each monotherapy group as demonstrated by flow cytometry analysis ($P > 0.05$) (Fig. 4A,B). Innate immunity plays a unique role in antitumor immunity [17,56–58]. In mice administered with PEG-IFNβ, the number of NK cells in B16F1 tumor significantly increased (0.83 ± 0.29 *vs.* 1.98 ± 0.73, $P < 0.01$) (Fig. 4C). Combination therapy induced an increase in antitumor innate immunity and T cell immunity, as indicated by the ratio of $CD8^+$T/Treg (2.59 ± 1.33 *vs* 5.71 ± 4.92, ns.), $CD8^+$T/$CD4^+$T (0.63 ± 0.22 *vs.* 1.97 ± 1.57, $P < 0.05$) (Fig. 4A,B), and the percentage of NK cells (0.83 %±0.29 *vs.* 1.81 %±0.45, $P < 0.05$) (Fig. 4C). No change in the number of tumor-infiltrating $CD3^+$T cells was detected by IHC in each monotherapy group, when compared with the vehicle-treated group. In sharp contrast, when PEG-IFNβ and anti-PD1 were administered simultaneously, the CD3-positive signal in tumor tissues significantly increased (Fig. 4D).

3.5. PEG-IFNβ exhibits superior growth inhibitory activity to PEG-IFNα-2b against human melanoma, NSCLC, and COAD cell lines

To further elucidate the clinically relevant biological function of PEG-IFNβ, the effect of PEG-IFNβ on the proliferative capacity of human melanoma cell line A375, NSCLC cell line A549, and COAD cell line HCT116 was evaluated via CCK-8 assay and clone formation assay. PEG-IFNα-2b was used as a comparator.

In the presence of a wide range of concentrations of PEG-IFNβ, a significant reduction in tumor cell growth rate was observed. Notably, PEG-IFNβ exhibited stronger tumor growth inhibitory ability than PEG-IFNα-2b in vitro, as demonstrated by the half-maximal inhibitory concentration (IC_{50}) for A375 (2312.0 ng/mL *vs.* 177.0 ng/mL) (Fig. 5A), A549 (78.9 ng/mL *vs.* 14.3 ng/mL) (Fig. 5B), and HCT116 (8093.0 ng/mL *vs.* 945.3 ng/mL) (Fig. 5C). These findings were further validated by clone formation assay, as indicated by the colony number for A375 (268.0 ± 23.1 *vs.* 202.8 ± 56.8), A549 (183.1 ± 23.1 *vs.* 84.3 ± 12.8), and HCT116 (372.5 ± 52.5 *vs.* 233.8 ± 27.6) (Fig. 5D).

3.6. PEG-IFNβ promotes human monocyte-derived DCs (MoDC) maturation more effectively than PEG-IFNα-2b

To investigate the role of PEG-IFNα-2b and PEG-IFNβ in regulating MoDC maturation, human PBMCs were cultured in the presence of GM-CSF (20 ng/mL) and IL-4 (160 ng/mL) to generate immature MoDC, which were subsequently treated with serial dilutions of PEG-IFNα-2b or PEG-IFNβ. Viable cells were sorted with 7-AAD negative areas and stained for $CD3^+CD14^+CD19^+CD20^+$ to exclude T cells, B cells and monocytes. DCs were gated based on HLA-DR and CD11c staining. Cell surface expression levels of DC maturation markers (CD80, CD83 and CD86), were subsequently measured by flow cytometry (Fig. 6A). Compared with PEG-IFNα-2b (50 ng/mL), PEG-IFNβ (50 ng/mL) showed a higher ability to promote the expression of DC maturation biomarkers, demonstrated by percentages of CD80 (4.10 % *vs.* 8.94 %), CD83 (5.74 % *vs.* 10.20 %), and CD86 (25.80 % *vs.* 37.90 %) positive MoDC subsets (Fig. 6B, Supplementary Table S1). These findings were further validated when MoDCs were cultured with PEG-IFNα-2b or PEG-IFNβ at different concentrations (50 – 400 ng/mL) (Fig. 6C). Our data suggests

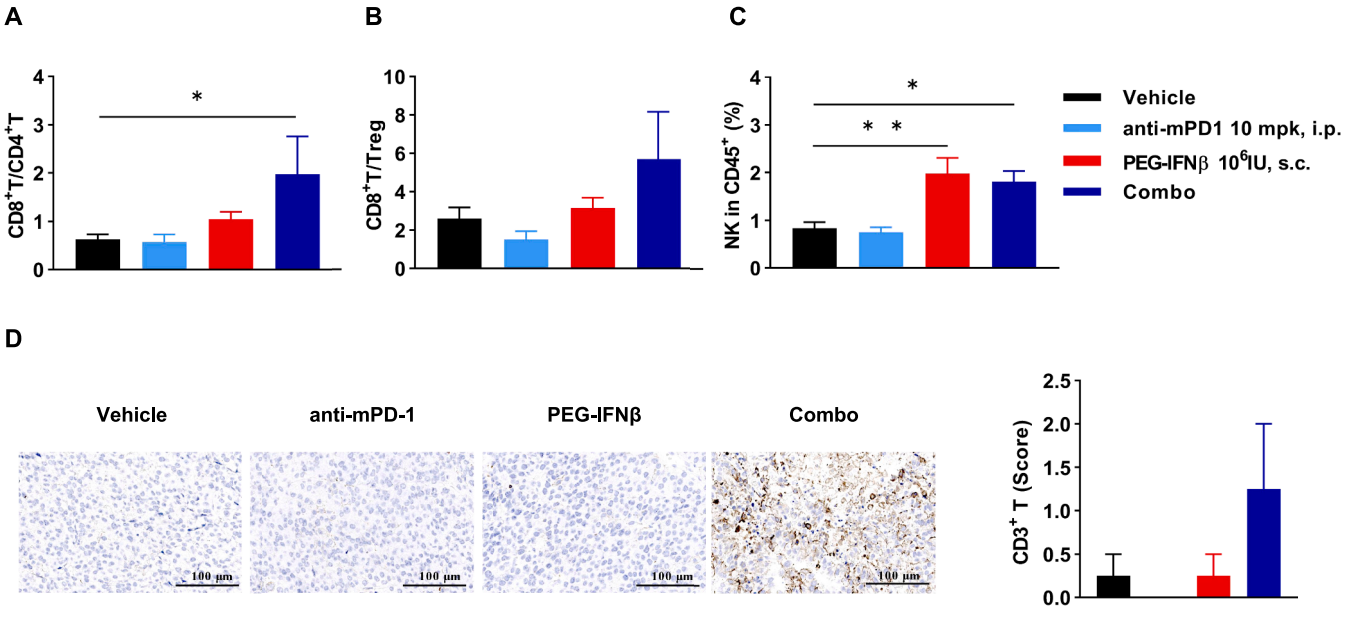

Fig. 4. Enhanced antitumor immunity mediated by PEG-IFNβ in the mouse B16F1 melanoma model. B16F1-bearing C57BL/6 mice (n = 6/group) were administered with PEG-IFNβ (s.c.) and anti-mPD-1 antibody (i.p.) on day 1 and day 4, as a single agent or in combination. Tumor tissues were isolated on day 6 and subjected to analysis of tumor infiltrating lymphocytes (TILs) by flow cytometry (**A, B, and C**) or $CD3^+$ T cells by IHC (**D**). *, $P < 0.05$; **, $P < 0.01$. Scale bar: 100 μm.

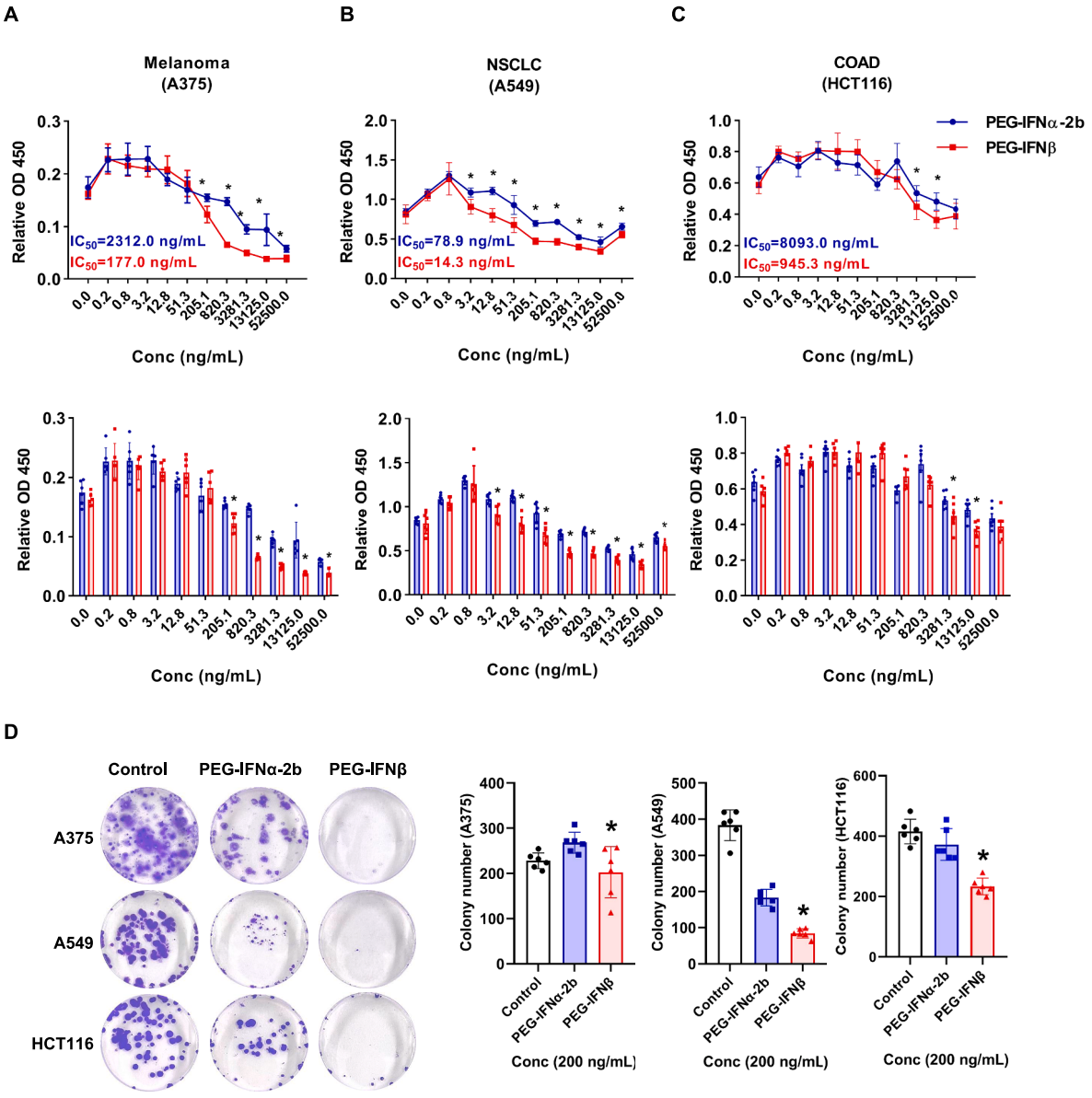

Fig. 5. PEG-IFNβ produces higher growth inhibitory activity against human melanoma, NSCLC, and COAD cell lines compared to PEG-IFNα-2b. Effects of PEG-IFNα-2b and PEG-IFNβ on the proliferation of A375 cells (**A**), A549 cells (**B**) and HCT116 cells (**C**). IC_{50}, half maximal inhibitory concentration. (**D**) Representative images of clone formation assay (left), and statistical analysis of colony number (right). Data are presented as mean ± SD. *, $P < 0.05$ (PEG-IFNβ *vs*. PEG-IFNα-2b).

that PEG-IFNβ promotes human MoDC maturation more effectively than PEG-IFNα-2b.

4. Discussion

Among type I Interferons, IFNα has been widely evaluated in cancer therapy, especially for the treatment of melanoma, either as monotherapy or in combination with ICIs. IFNα combined with anti-CTLA-4 immunotherapy produced acceptable safety and promising clinical activity in patients with metastatic melanoma in a phase II trial [59]. Phase I/II trials with anti-PD-1 plus PEG-IFNα combination demonstrated more activated tumour-reactive T cells, leading to improved clinical outcomes in patients with metastatic melanoma [59,60]. Co-administration with Pembrolizumab and IFNα-2b in patients with resectable stage III/IV melanoma showed a manageable safety profile with improved overall response rate (73.3 %) and pathologic complete response rate (43 %), superior to IFNα-2b monotherapy [61]. A neo-adjuvant, consisting of Ipilimumab and IFNα-2b, has been used to treat patients with locally/regionally advanced melanoma with a favorable safety profiles and promising response rates [17,62].

In terms of antitumor therapy, preliminary data showed that IFNβ exhibited superior antitumor potency to IFNα, which may be attribute in part to the enhanced potency of IFNβ in receptor binding [17,27], tumor cell growth inhibition and apoptosis induction [24–26], DCs activation [17,28], and angiogenesis inhibition [29] as shown by comparative in vitro assessments of human IFNα and IFNβ. A recent in vivo analysis of mouse IFNα and IFNβ suggests that IFNβ may be a better adjuvant than several subtypes of IFNα [63].

In the current study, we investigated the in vivo antitumor efficacy of PEG-IFNβ as monotherapy or in combination with anti-PD-1 antibodies in three syngeneic mouse tumor models (melanoma, NSCLC, and COAD). Although mIFNβ does not show anti-proliferative effect on human tumor cells due to limited cross-species activity [64]. hIFNβ exhibited weak but definite cross-species activity in mice (Fig. 1). The same conclusion has been reached as indicated by preclinical studies of hIFNβ (such as Rebif®) in experimental autoimmune encephalomyelitis

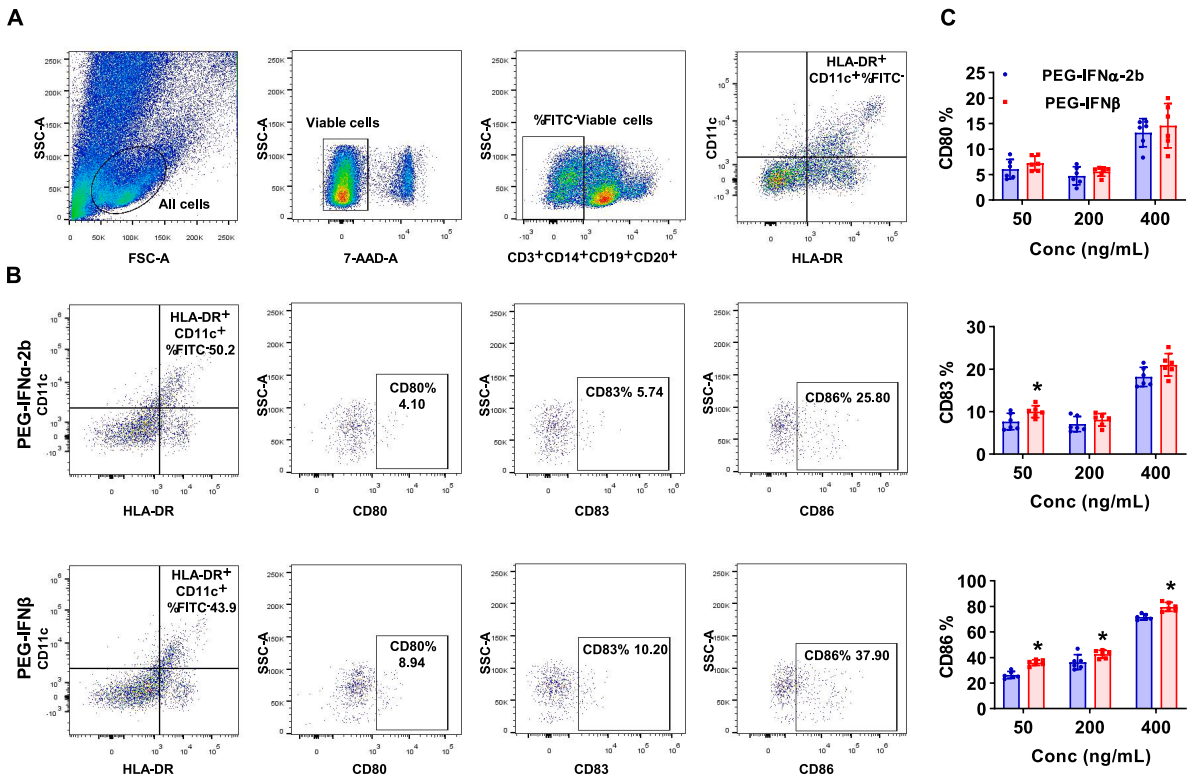

Fig. 6. PEG-IFNβ enhanced cell surface expression of human MoDC maturation markers more efficiently than PEG-IFNα-2b. (**A**) Flow sort diagram image of MoDCs. (**B**) Flow histogram images of CD80, CD83 and CD86 expressed on MoDCs treated by PEG-IFNα-2b or PEG-IFNβ (50 ng/mL). Representative results of 6 independent experiments. (**C**) The expression levels of CD80, CD83 and CD86 on MoDCs, cocultured with PEG-IFNα-2b or PEG-IFNβ (50 – 400 ng/mL) determined by flow cytometry.

(EAE) mouse model [65] and syngeneic murine melanoma model [66]. PEG-IFNβ as a single agent slowed tumor cell growth in vivo in all models (Fig. 2), and enhanced the antitumor benefit of ICIs in a combination setting (Fig. 3). These findings validate the conclusions when mIFNβ was used for treatment in mouse melanoma models [37,38,63].

Furthermore, administration of PEG-IFNβ at high dose levels (10^7 IU, equal to 5.8 mg/kg) induced only moderate responses compared to mIFNβ (0.1 mpk) (Fig. 1). Future studies are necessary to accurately elucidate the dose–response relationship of PEG-IFNβ, and the antitumor effects of different IFN signaling strengths (hIFNα *vs*. hIFNβ) in mouse models carrying human type I interferon receptors (IFNARs), such as human IFNAR transgenic mice [17,50], which was not available at the time of this study. Xenograft models based on mice with a functional humanized immune system might be an alternative approach to comprehensively understand how hIFNβ modulates the anti-tumor immune responses. Furthermore, since syngeneic mouse models are immunogenic differently than human tumors of the same tissue origin [67], further studies based on patient-derived xenograft (PDX) models may provide more additional clinically relevant implications for clinical translation.

The synergistic suppression of tumor growth by combination treatment with ICIs and PEG-IFNβ can be partially attributed to $CD8^+$ T cells and NK cells, since the cause-and-effect relationship between intratumoral effector cells and tumor suppression after treatment with IFN-β or ICIs has been comprehensively clarified by previous research through antibody-mediated depletion of T cells or NK cells [64,68–70]. Increased presence of intratumoral effector cells confirmed the above findings (Fig. 4).

In vitro comparative study between PEG-IFNβ and PEG-IFNα-2b demonstrated superior activity of PEG-IFNβ in inhibiting human tumor cell proliferation (Fig. 5) and activating human MoDCs (Fig. 6), in alignment with previously reported findings [27,28]. Anti-angiogenic activity, another approach used by type I IFNs to inhibit tumor development [14], has been evaluated comparatively between hIFNα and hIFNβ [29] but was not explored in this study. Cytokines can be pleiotropic [71] and the impact of type I IFN signaling strength on antitumor effects is context-dependent [17,72]. In a clinical setting, the baseline strength of the type I IFN signal should be noted and incorporated into the evaluation of treatment modalities including type I IFN therapy.

In conclusion, our study demonstrates the antitumor activity of PEG-IFNβ as monotherapy or in combination with ICIs. PEG-IFNβ exhibits greater potency in human tumor growth inhibition and human MoDC activation compared to PEG-IFNα-2b. Future application of PEG-IFNβ in clinical settings should be further evaluated.

CRediT authorship contribution statement

Rui Wang: Conceptualization, Investigation, Validation, Visualization, Writing – original draft, Writing – review & editing. **Tao Zhang:** Investigation, Data curation, Formal analysis, Visualization, Writing – original draft. **Yuan Lu:** Investigation, Data curation, Formal analysis, Visualization, Writing – original draft. **Yalong Lin:** Investigation, Data curation. **Shuyuan Kou:** Investigation, Data curation. **Xuefeng Li:** Writing – review & editing. **Yang Wang:** Writing – review & editing. **Liangzhi Xie:** Supervision, Funding acquisition, Project administration, Conceptualization, Writing – original draft, Writing – review & editing.

Declaration of Competing Interest

The authors declare that they have no known competing financial interests or personal relationships that could have appeared to influence the work reported in this paper.

Data availability

Data will be made available on request.

Acknowledgements

This work was funded by Sinocelltech Ltd., with support from National Major Scientific and Technological Special Project for "Significant New Drugs Development" (No. 2017ZX09303005).

Appendix A. Supplementary data

Supplementary data to this article can be found online at https://doi.org/10.1016/j.cellimm.2023.104782.

References

[1] H.F. Tsai, P.N. Hsu, Cancer immunotherapy by targeting immune checkpoints: mechanism of T cell dysfunction in cancer immunity and new therapeutic targets, J. Biomed. Sci. 24 (1) (2017) 35, https://doi.org/10.1186/s12929-017-0341-0.
[2] K. Ganesh, et al., Immunotherapy in colorectal cancer: rationale, challenges and potential, Nat. Rev. Gastroenterol. Hepatol. 16 (6) (2019) 361–375, https://doi.org/10.1038/s41575-019-0126-x.
[3] A. Derakhshani, et al., From oncogenic signaling pathways to single-cell sequencing of immune cells: changing the landscape of cancer immunotherapy, Molecules 26 (8) (2021), https://doi.org/10.3390/molecules26082278.
[4] O. Kooshkaki, et al., The latest findings of PD-1/PD-L1 inhibitor application in gynecologic cancers, Int. J. Mol. Sci. 21 (14) (2020), https://doi.org/10.3390/ijms21145034.
[5] T.K. Kim, R.S. Herbst, L. Chen, Defining and Understanding Adaptive Resistance in Cancer Immunotherapy, Trends Immunol. 39 (8) (2018) 624–631, https://doi.org/10.1016/j.it.2018.05.001.
[6] S.P. Kubli, et al., Beyond immune checkpoint blockade: emerging immunological strategies, Nat. Rev. Drug Discov. 20 (12) (2021) 899–919, https://doi.org/10.1038/s41573-021-00155-y.
[7] L. Kraehenbuehl, et al., Enhancing immunotherapy in cancer by targeting emerging immunomodulatory pathways, Nat. Rev. Clin. Oncol. 19 (1) (2022) 37–50, https://doi.org/10.1038/s41571-021-00552-7.
[8] S. Spranger, T.F. Gajewski, Impact of oncogenic pathways on evasion of antitumour immune responses, Nat. Rev. Cancer 18 (3) (2018) 139–147, https://doi.org/10.1038/nrc.2017.117.
[9] M.A. Postow, et al., Nivolumab and ipilimumab versus ipilimumab in untreated melanoma, N. Engl. J. Med. 372 (21) (2015) 2006–2017, https://doi.org/10.1056/NEJMoa1414428.
[10] J.E. Rosenberg, et al., Atezolizumab in patients with locally advanced and metastatic urothelial carcinoma who have progressed following treatment with platinum-based chemotherapy: a single-arm, multicentre, phase 2 trial, Lancet 387 (10031) (2016) 1909–1920, https://doi.org/10.1016/S0140-6736(16)00561-4.
[11] A. Haslam, V. Prasad, Estimation of the percentage of US patients with cancer who are eligible for and respond to checkpoint inhibitor immunotherapy drugs, JAMA Netw. Open 2 (5) (2019) e192535.
[12] B. Zhao, H. Zhao, J. Zhao, Efficacy of PD-1/PD-L1 blockade monotherapy in clinical trials, Ther. Adv. Med. Oncol. 12 (2020), https://doi.org/10.1177/1758835920937612, p. 1758835920937612.
[13] J.D. Wolchok, et al., Overall survival with combined nivolumab and ipilimumab in advanced melanoma, N. Engl. J. Med. 377 (14) (2017) 1345–1356, https://doi.org/10.1056/NEJMoa1709684.
[14] E.C. Borden, Interferons alpha and beta in cancer: therapeutic opportunities from new insights, Nat. Rev. Drug Discov. 18 (3) (2019) 219–234, https://doi.org/10.1038/s41573-018-0011-2.
[15] R. Yu, B. Zhu, D. Chen, Type I interferon-mediated tumor immunity and its role in immunotherapy, Cell. Mol. Life Sci. 79 (3) (2022) 191, https://doi.org/10.1007/s00018-022-04219-z.
[16] L. Zitvogel, et al., Type I interferons in anticancer immunity, Nat. Rev. Immunol. 15 (7) (2015) 405–414, https://doi.org/10.1038/nri3845.
[17] C.S. Garris, et al., Successful anti-PD-1 cancer immunotherapy requires T cell-dendritic cell crosstalk involving the cytokines IFN-γ and IL-12, Immunity 49 (6) (2018) 1148–1161.e7, https://doi.org/10.1016/j.immuni.2018.09.024.
[18] M. De Palma, et al., Tumor-targeted interferon-alpha delivery by Tie2-expressing monocytes inhibits tumor growth and metastasis, Cancer Cell 14 (4) (2008) 299–311, https://doi.org/10.1016/j.ccr.2008.09.004.
[19] J. Sprooten, P. Agostinis, A.D. Garg, Type I interferons and dendritic cells in cancer immunotherapy, Int. Rev. Cell Mol. Biol. 348 (2019) 217–262, https://doi.org/10.1016/bs.ircmb.2019.06.001.
[20] B.S. Parker, J. Rautela, P.J. Hertzog, Antitumour actions of interferons: implications for cancer therapy, Nat. Rev. Cancer 16 (3) (2016) 131–144, https://doi.org/10.1038/nrc.2016.14.
[21] J.R. Quesada, et al., Alpha interferon for induction of remission in hairy-cell leukemia, N. Engl. J. Med. 310 (1) (1984) 15–18, https://doi.org/10.1056/NEJM198401053100104.
[22] A.M. Eggermont, et al., Adjuvant therapy with pegylated interferon alfa-2b versus observation alone in resected stage III melanoma: final results of EORTC 18991, a randomised phase III trial, Lancet 372 (9633) (2008) 117–126, https://doi.org/10.1016/S0140-6736(08)61033-8.
[23] T.M. Herndon, U.s., et al., Food and Drug Administration Approval: peginterferon-alfa-2b for the adjuvant treatment of patients with melanoma, Oncologist 17 (10) (2012) 1323–1328, https://doi.org/10.1634/theoncologist.2012-0123.
[24] T.F. Gajewski, L. Corrales, New perspectives on type I IFNs in cancer, Cytokine Growth Factor Rev. 26 (2) (2015) 175–178, https://doi.org/10.1016/j.cytogfr.2015.01.001.
[25] H. Zhang, et al., Induction of multiple programmed cell death pathways by IFN-beta in human non-small-cell lung cancer cell lines, Exp. Cell Res. 247 (1) (1999) 133–141, https://doi.org/10.1006/excr.1998.4329.
[26] S. Yoshimura, et al., IFN-beta sensitizes TRAIL-induced apoptosis by upregulation of death receptor 5 in malignant glioma cells, Oncol. Rep. 42 (6) (2019) 2635–2643, https://doi.org/10.3892/or.2019.7383.
[27] C.T. Ng, et al., Alpha and beta type 1 interferon signaling: passage for diverse biologic outcomes, Cell 164 (3) (2016) 349–352, https://doi.org/10.1016/j.cell.2015.12.027.
[28] B.M. Hartmann, et al., Combinatorial cytokine code generates anti-viral state in dendritic cells, Front. Immunol. 5 (2014) 73, https://doi.org/10.3389/fimmu.2014.00073.
[29] H. Enomoto, et al., The in vivo antitumor effects of type I-interferon against hepatocellular carcinoma: the suppression of tumor cell growth and angiogenesis, Sci. Rep. 7 (1) (2017) 12189, https://doi.org/10.1038/s41598-017-12414-3.
[30] G. Varyte, A. Arlauskiene, D. Ramasauskaite, Pregnancy and multiple sclerosis: an update, Curr. Opin. Obstet. Gynecol. 33 (5) (2021) 378–383, https://doi.org/10.1097/GCO.0000000000000731.
[31] D. Jakimovski, et al., Interferon beta for multiple sclerosis, Cold Spring Harb. Perspect. Med. 8 (2018), https://doi.org/10.1101/cshperspect.a032003.
[32] T. Yanagi, et al., Adjuvant therapy with low-dose interferon-beta for stage II and III melanoma: results of a retrospective analysis, Clin. Exp. Dermatol. 42 (7) (2017) 781–785, https://doi.org/10.1111/ced.13179.
[33] S. Aoyagi, et al., Sequential local injection of low-dose interferon-beta for maintenance therapy in stage II and III melanoma: a single-institution matched case-control study, Oncology 82 (3) (2012) 139–146, https://doi.org/10.1159/000336490.
[34] K. Namikawa, et al., Randomized phase III trial of adjuvant therapy with locoregional interferon beta versus surgery alone in stage II/III cutaneous melanoma: japan clinical oncology group study (JCOG1309, J-FERON), Jpn. J. Clin. Oncol. 47 (7) (2017) 664–667, https://doi.org/10.1093/jjco/hyx063.
[35] K. Namikawa, N. Yamazaki, Targeted therapy and immunotherapy for melanoma in japan, Curr. Treat. Options Oncol. 20 (1) (2019) 7, https://doi.org/10.1007/s11864-019-0607-8.
[36] T. Fujimura, et al., Phase I study of nivolumab combined with IFN-beta for patients with advanced melanoma, Oncotarget 8 (41) (2017) 71181–71187, https://doi.org/10.18632/oncotarget.17090.
[37] A. Kakizaki, et al., Immunomodulatory effect of peritumorally administered interferon-beta on melanoma through tumor-associated macrophages, Oncoimmunology 4 (11) (2015) e1047584.
[38] J. Uehara, et al., Intratumoral injection of IFN-beta induces chemokine production in melanoma and augments the therapeutic efficacy of anti-PD-L1 mAb, Biochem. Biophys. Res. Commun. 490 (2) (2017) 521–527, https://doi.org/10.1016/j.bbrc.2017.06.072.
[39] B.C. Kieseier, P.A. Calabresi, PEGylation of interferon-beta-1a: a promising strategy in multiple sclerosis, CNS Drugs 26 (3) (2012) 205–214, https://doi.org/10.2165/11596970-000000000-00000.
[40] M. Tsuge, et al., Development of a Novel Site-Specific Pegylated Interferon Beta for Antiviral Therapy of Chronic Hepatitis B Virus, Antimicrob. Agents Chemother. 61 (6) (2017), https://doi.org/10.1128/AAC.00183-17.
[41] J. Jablonska, et al., CXCR2-mediated tumor-associated neutrophil recruitment is regulated by IFN-beta, Int. J. Cancer 134 (6) (2014) 1346–1358, https://doi.org/10.1002/ijc.28551.
[42] M. Severa, et al., Differential responsiveness to IFN-alpha and IFN-beta of human mature DC through modulation of IFNAR expression, J. Leukoc. Biol. 79 (6) (2006) 1286–1294, https://doi.org/10.1189/jlb.1205742.
[43] A. Antonelli, et al., Interferon-alpha, -beta and -gamma induce CXCL9 and CXCL10 secretion by human thyrocytes: modulation by peroxisome proliferator-activated receptor-gamma agonists, Cytokine 50 (3) (2010) 260–267, https://doi.org/10.1016/j.cyto.2010.01.009.
[44] C. Zhukovsky, et al., Urokinase, CX3CL1, CCL2, TRAIL and IL-18 induced by interferon-beta treatment, Acta Neurol. Scand. 143 (6) (2021) 602–607, https://doi.org/10.1111/ane.13400.
[45] E.C. Borden, et al., Gene regulatory and clinical effects of interferon beta in patients with metastatic melanoma: a phase II trial, J. Interferon Cytokine Res. 31 (5) (2011) 433–440, https://doi.org/10.1089/jir.2010.0054.
[46] B.K. Paap, et al., An inventory of short term and long term changes in gene expression under interferon beta treatment of relapsing remitting MS patients, Curr. Pharm. Des. 18 (29) (2012) 4475–4484, https://doi.org/10.2174/138161212802502215.
[47] C. Bossard, et al., Immunohistochemistry as a valuable tool to assess CD30 expression in peripheral T-cell lymphomas: high correlation with mRNA levels, Blood 124 (19) (2014) 2983–2986, https://doi.org/10.1182/blood-2014-07-584953.

[48] A. Uguen, et al., A p16-Ki-67-HMB45 immunohistochemistry scoring system as an ancillary diagnostic tool in the diagnosis of melanoma, Diagn. Pathol. 10 (2015) 195, https://doi.org/10.1186/s13000-015-0431-9.
[49] *Blast*. Available from: https://blast.ncbi.nlm.nih.gov/Blast.cgi.
[50] D. Harari, et al., Bridging the species divide: transgenic mice humanized for type-I interferon response, PLoS One 9 (1) (2014) e84259.
[51] M.G. Lechner, et al., Immunogenicity of murine solid tumor models as a defining feature of in vivo behavior and response to immunotherapy, J. Immunother. 36 (9) (2013) 477–489, https://doi.org/10.1097/01.cji.0000436722.46675.4a.
[52] S.I. Mosely, et al., Rational selection of syngeneic preclinical tumor models for immunotherapeutic drug discovery, Cancer Immunol. Res. 5 (1) (2017) 29–41, https://doi.org/10.1158/2326-6066.CIR-16-0114.
[53] G. Fierlbeck, et al., Pharmacodynamics of recombinant IFN-beta during long-term treatment of malignant melanoma, J. Interferon Cytokine Res. 16 (10) (1996) 777–781, https://doi.org/10.1089/jir.1996.16.777.
[54] S. Song, et al., Tumour-derived IL-10 within tumour microenvironment represses the antitumour immunity of Socs1-silenced and sustained antigen expressing DCs, Eur. J. Cancer 48 (14) (2012) 2252–2259, https://doi.org/10.1016/j.ejca.2011.12.009.
[55] N. Shi, et al., PD-1/LAG-3 bispecific antibody potentiates T cell activation and increases antitumor efficacy, Front. Immunol. 13 (2022) 1047610, https://doi.org/10.3389/fimmu.2022.1047610.
[56] E.C. Toffoli, et al., Natural killer cells and anti-cancer therapies: reciprocal effects on immune function and therapeutic response, Cancers (basel) 13 (4) (2021), https://doi.org/10.3390/cancers13040711.
[57] A.S. Chretien, N. Dulphy, E. Marcenaro, Editorial: innate anti-tumor immune responses in solid and hematological malignancies: from basic research to clinical applications, Front. Immunol. 13 (2022), 957119, https://doi.org/10.3389/fimmu.2022.957119.
[58] T.F. Gajewski, H. Schreiber, Y.X. Fu, Innate and adaptive immune cells in the tumor microenvironment, Nat. Immunol. 14 (10) (2013) 1014–1022, https://doi.org/10.1038/ni.2703.
[59] I. Rafique, J.M. Kirkwood, A.A. Tarhini, Immune checkpoint blockade and interferon-alpha in melanoma, Semin. Oncol. 42 (3) (2015) 436–447, https://doi.org/10.1053/j.seminoncol.2015.02.012.
[60] M.K. van der Kooij, et al., Phase I/II study protocol to assess safety and efficacy of adoptive cell therapy with anti-PD-1 plus low-dose pegylated-interferon-alpha in patients with metastatic melanoma refractory to standard of care treatments: the ACTME trial, BMJ Open 10 (11) (2020) e044036.
[61] Najjar, Y.G., D. McCurry, and H. Lin, *Neoadjuvant Pembrolizumab and High-Dose IFNα-2b in Resectable Regionally Advanced Melanoma.* 2021. **27**(15): p. 4195-4204. http://doi.org/10.1158/1078-0432.ccr-20-4301.
[62] A. Tarhini, et al., Neoadjuvant ipilimumab (3 mg/kg or 10 mg/kg) and high dose IFN-alpha2b in locally/regionally advanced melanoma: safety, efficacy and impact on T-cell repertoire, J. Immunother. Cancer 6 (1) (2018) 112, https://doi.org/10.1186/s40425-018-0428-5.
[63] K.M. Audsley, et al., IFNbeta Is a potent adjuvant for cancer vaccination strategies, Front. Immunol. 12 (2021), 735133, https://doi.org/10.3389/fimmu.2021.735133.
[64] X.Q. Qin, et al., Human and mouse IFN-beta gene therapy exhibits different anti-tumor mechanisms in mouse models, Mol. Ther. 4 (4) (2001) 356–364, https://doi.org/10.1006/mthe.2001.0464.
[65] Rajendran, R. and V. Rajendran, Interferon Beta-1a versus Combined Interferon Beta-1a and Oligodendrocyte-Specific FGFR1 Deletion in Experimental Autoimmune Encephalomyelitis. 2022. **23**(20). http://doi.org/10.3390/ijms232012183.
[66] C.J. Streck, et al., Antitumor efficacy of AAV-mediated systemic delivery of interferon-beta, Cancer Gene Ther. 13 (1) (2006) 99–106, https://doi.org/10.1038/sj.cgt.7700878.
[67] W. Zhong, et al., Comparison of the molecular and cellular phenotypes of common mouse syngeneic models with human tumors, BMC Genomics 21 (1) (2020) 2, https://doi.org/10.1186/s12864-019-6344-3.
[68] Tseng, S.H., et al., Albumin and interferon-β fusion protein serves as an effective vaccine adjuvant to enhance antigen-specific CD8+ T cell-mediated antitumor immunity. 2022. **10**(4). http://doi.org/10.1136/jitc-2021-004342.
[69] Y. Ma, et al., Combination of PD-1 inhibitor and OX40 agonist induces tumor rejection and immune memory in mouse models of pancreatic cancer, Gastroenterology 159 (1) (2020) 306–319.e12, https://doi.org/10.1053/j.gastro.2020.03.018.
[70] M. Wang, et al., Humanized mice in studying efficacy and mechanisms of PD-1-targeted cancer immunotherapy, FASEB J. 32 (3) (2018) 1537–1549, https://doi.org/10.1096/fj.201700740R.
[71] P.G. Holder, et al., Engineering interferons and interleukins for cancer immunotherapy, Adv. Drug Deliv. Rev. 182 (2022), 114112, https://doi.org/10.1016/j.addr.2022.114112.
[72] E.A. Lutz, et al., Alum-anchored intratumoral retention improves the tolerability and antitumor efficacy of type I interferon therapies, Proc. Natl. Acad. Sci. USA 119 (36) (2022), https://doi.org/10.1073/pnas.2205983119.